

Switched Delay Line Reconfigurable Microwave Filter

Peng Wen Wong, Ian Hunter

Institute of Microwaves and Photonics, School of Electronic and Electrical Engineering,
University of Leeds, Leeds, LS2 9JT, UK

Abstract

A novel electronically reconfigurable microwave bandpass filter based on switched delay line approach is presented. In contrast to conventional tunable filters, the approach enables the lossy and non-linear switching elements to be used as part of the coupling elements rather than within the resonators. Therefore the filter distinguishes itself through its ability to provide a wide tuning bandwidth with low passband loss and high linearity. Theoretical analysis of the approach is presented in this paper. The feasibility of the approach has been experimentally verified with microstrip circuit prototype. The filter produced a maximum passband loss of 1.7 dB and an IP3 of >32 dBm with 35% tuning bandwidth.

Introduction

Modern high frequency system designs must simultaneously support multiple frequency bands. This results in stringent demands on adaptive front-end electronics where tunable filters are highly desirable. As a consequence of the continuing evolution of miniaturized microwave systems which leads to planar and MMIC integration, electronically tunable microwave filters offer the great advantages of small size, light weight and fast tuning capability. Although different realizations of electronically tunable filters have been developed over the past decades, most prior work has been concentrating on tuning the resonant frequency of the resonators either in continuous or discrete fashion using semiconductor, ferroelectric or micro-electromechanical systems (MEMs) varactors [1]-[8]. Such tunable filters exhibit high losses and poor linearity due to the varactor nonlinearity. Alternatively, the technique of integrating the active devices into the tunable filter design for loss compensation has been proposed and

investigated [9]-[13]. Although the loss compensation technique would be useful in small signal conditions to restore the shape of the filter response, there are other nonlinear-related problems such as intermodulation distortion as in reality the tunable filter has multiple inputs with potentially high power [1]. Therefore the disadvantages of the conventional approach has made it apparent that a new technique for realizing electronically reconfigurable microwave filters has to be developed where the filter should have low loss, high linearity and wide frequency tuning bandwidth.

A completely new approach to realize a microwave tunable filter based on switched delay line is reported here. The theory describing the switched delay line approach is presented which validates the feasibility of a wide resonant frequency tuning range by simply toggling the position of the output switches. This is followed by the introduction of a multi-section filter where the basic switched delay line resonators are cascaded to realize quasi-elliptic filter

response. Theory of introducing a control element to improve the inherent transfer characteristic is also presented. Finally, experimental prototypes are realized to demonstrate the feasibility of the approach and measurements of linear and nonlinear performance are presented.

Theory

A. Switched delay line resonator and resonant tuning methodology

Consider the filter structure shown in Fig.1, consisting of a power splitter which divides the incident signal between two parallel delay lines, and a multi-pole RF switch that combines the signals at the output. The voltage at the output point P is,

$$V_p = \frac{V}{\sqrt{2}} \left(\frac{e^{-j\theta_1} + e^{-j\theta_2}}{2} \right) \quad (1)$$

and therefore $|V_p|$ is given by,

$$|V_p| = \frac{V}{\sqrt{2}} \cos\left(\frac{\theta}{2}\right) \quad (2)$$

where $\theta = \theta_2 - \theta_1$. It should be noted that the impedance seen at the output port is now half of the system impedance since the delay lines are connected in parallel. First assume that the output is terminated with a matched load where the output reflection coefficient is given by,

$$|S_{22}(\omega)| = 0 \quad (3)$$

The transfer function is derived as,

$$\begin{aligned} |S_{21}|^2 &= \frac{\text{Power delivered to load}}{\text{Power available from source}} \\ &= \frac{|V_p|^2}{\frac{Z_o}{2}} = \cos^2\left(\frac{\theta}{2}\right) \end{aligned} \quad (4)$$

Let the relative phase in the two paths be

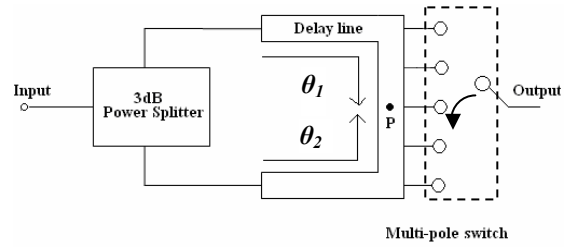


Fig. 1. Switched delay line resonator.

$$\theta = \frac{\pi\omega}{\omega_o} \quad (5)$$

where $\theta = \Pi$ when $\omega = \omega_o$. The transmission response of the corresponding switched delay line resonator is shown in Fig. 2. The phase relationship between the delay lines can be engineered by toggling the output switch to the appropriate position such that the desired stopband edges and passband are defined by destructive and constructive signal interference. Therefore, a very wide tuning bandwidth is achievable by simply toggling the output switch.

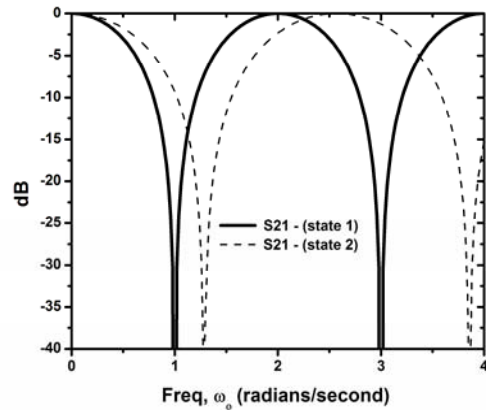


Fig. 2. Transmission responses of switched delay line resonator with toggled output switch at point P (solid line) or at position with 20 degree electrical length away from point P (dotted line).

B. Quasi-elliptic filter response

Consider a two-stage filter by cascading the basic switched delay line resonator with a second resonator section in which the length of the delay line is doubled. The overall transfer function is given by,

$$|S_{21}(\omega)|^2 = \cos^2\left(\frac{\theta}{2}\right) \cos^2(\theta) \quad (6)$$

Now since,

$$\begin{aligned} \cos\left(\frac{N\theta}{2}\right) &= \cos\left[N \cos^{-1}\left(\cos\frac{\theta}{2}\right)\right] \\ &= T_N\left[\cos\left(\frac{\theta}{2}\right)\right] \end{aligned} \quad (7)$$

where T_N is a chebyshev polynomial in terms of $\cos\left(\frac{\theta}{2}\right)$. Hence the transfer

characteristic due to the second resonator section may be shown as,

$$\cos(\theta) = T_2\left[\cos\left(\frac{\theta}{2}\right)\right] = 2 \cos^2\left(\frac{\theta}{2}\right) - 1 \quad (8)$$

where the additional transmission zeros are introduced at both passband edges when $T_2 = 0$ which yield a quasi-elliptic function filter response as shown in Fig. 3. In general an N -stage filter could be realized to produce additional transmission zeros where the transfer function may be expressed by,

$$|S_{21}(\omega)|^2 = \left| \prod_{r=1}^N T_N\left(\cos\frac{\theta}{2}\right) \right|^2 \quad (9)$$

C. Passband bandwidth and stopband ripple level

The filter's frequency response is entirely determined by the product of the chebyshev polynomials as shown in (9). The 3dB passband bandwidth can be obtained by letting $|S_{21}(\omega)|^2 = \frac{1}{2}$. Let's consider the case $N=2$, the delay lines length of the second resonator section is doubled where the phase difference changes more rapidly with frequency. Hence the passband bandwidth is mainly determined by the second switched delay line resonator section. Therefore a good approximation could be made where the 3dB point is found by solving the equation,

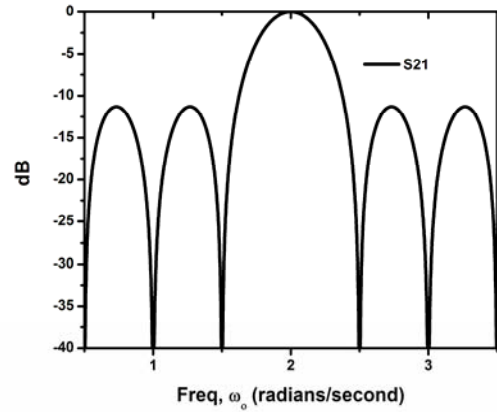


Fig. 3. Quasi-elliptic function filter response.

$$\cos^2\left(N \frac{\theta}{2}\right) = 0.5 \quad (10)$$

and the filter's 3dB frequency is given by,

$$\omega_{3dB} \approx \frac{\omega_o}{2N} \quad (11)$$

To determine the stopband ripple level, consider the transmission coefficient of a N -stage switched delay line filter which is given by,

$$|S_{21}(\omega)| = P_N(x) = \left| \prod_{r=1}^N \cos(Nx) \right| \quad (12)$$

where $x = \frac{\theta}{2}$. For $N=2$,

$$P_2(x) = |\cos(x) \cos(2x)| \quad (13)$$

Differentiating $P_2(x)$ with respect to x and equating to zero gives,

$$\left. \frac{dP_2(x)}{dx} \right|_0 = \tan(X_m) + 2 \tan(2X_m) \quad (14)$$

where $P_2(x)$ possesses maximum ripple when $x = X_m$. Now for $N=3$,

$$\begin{aligned} \left. \frac{dP_3(x)}{dx} \right|_0 &= \tan(X_m) + 2 \tan(2X_m) \\ &+ 3 \tan(3X_m) \end{aligned} \quad (15)$$

Therefore it can be deduced that,

$$\left. \frac{d|S_{21}(\omega)|}{d(\theta/2)} \right|_{\theta=0} = \sum_{r=1}^N N \tan\left(N \frac{\theta_m}{2}\right) \quad (16)$$

where $S_{21}(\omega)$ possesses maximum ripple when $\theta = \theta_m$. Now since,

$$\sum_{r=1}^N N \tan\left(N \frac{\theta_m}{2}\right) = \tan \frac{\theta_m}{2} \frac{N \left(\tan \frac{\theta_m}{2}\right)}{D\left(\tan \frac{\theta_m}{2}\right)} \quad (17)$$

where the numerator $N\left(\tan \frac{\theta_m}{2}\right)$ is a polynomial in terms of $\tan \frac{\theta_m}{2}$. By solving the polynomial $N\left(\tan \frac{\theta_m}{2}\right)$ and substituting θ_m into (9), the stopband ripple level R is given by,

$$R(dB) = 10 \log\left(\frac{1}{|S_{21}(\theta_m)|^2}\right) \quad (18)$$

For example for $N=2$,

$$\left. \frac{d|S_{21}(\omega)|}{d(\theta/2)} \right|_{\theta=0} = \tan\left(\frac{\theta_m}{2}\right) + 2 \tan\left(2 \frac{\theta_m}{2}\right) \quad (19)$$

and,

$$N\left(\tan \frac{\theta_m}{2}\right) = 5 - \tan^2\left(\frac{\theta_m}{2}\right) \quad (20)$$

By solving (20) we obtain $\theta_m = 131.8^\circ$ and hence the stopband ripple level $R = 11.3 \text{ dB}$.

D. Introduction of passband bandwidth and stopband rejection control element

To improve both passband bandwidth and stopband rejection further, a modified switched delay line circuit configuration as shown in Fig. 4 is proposed where an extra control element is introduced. Two basic switched delay line resonator sections are cascaded in reverse direction via a unit element (quarter-wave-long transmission-line element). The transfer matrix of a unit element is given by,

$$[T] = \frac{1}{(1-t^2)^{1/2}} \begin{bmatrix} 1 & Zt \\ Yt & 1 \end{bmatrix} \quad (21)$$

where $t = j \tan\left(\frac{\pi f}{2 f_o}\right)$ and Z is the characteristic impedance of the unit element normalized to $Z_o/2$. The transmission coefficient S_{21} is given by,

$$S_{21} = \frac{2}{A+B+C+D} \quad (22)$$

Although the second resonator section is placed in reverse direction, the transfer characteristic still remains unchanged except for $\frac{\theta}{2} \rightarrow \theta$ as it is a reciprocal network. Hence the overall transfer function may be derived as,

$$|S_{21}(\omega)|^2 = A(\omega, Z) \left[\cos^2\left(\frac{\theta}{2}\right) \cos^2(\theta) \right] \quad (23)$$

and,

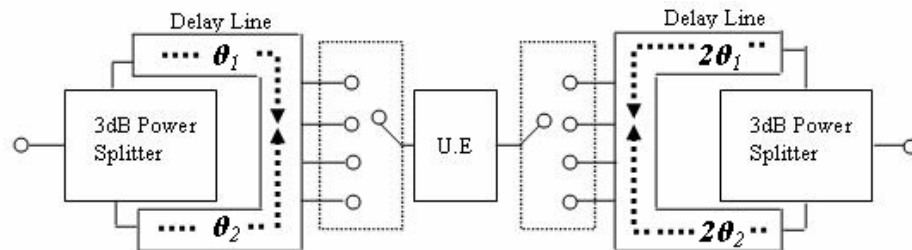


Fig. 4. Two-stage switched delay line circuit configuration with passband bandwidth and stopband rejection control element.

$$A(\omega, Z) = \frac{4 \left[1 + \tan^2 \left(\frac{\pi \omega}{2 \omega_o} \right) \right]}{4 + \left(Z + \frac{1}{Z} \right)^2 \tan^2 \left(\frac{\pi \omega}{2 \omega_o} \right)} \quad (24)$$

An additional control element $A(\omega, Z)$ is now introduced as part of the transfer function which enables the control of passband bandwidth and stopband ripple level without affecting the filter's transmission poles or zeros. It is important to notice that if $f = 2f_o$,

$$A(\omega, Z) = 1 \quad (25)$$

hence a transmission pole is obtained as $T_N(1) = 1$ for all chebyshev polynomials.

To improve the passband bandwidth and stopband ripple level, let's first evaluate the passband response by considering $f \rightarrow 2f_o$, the complex frequency t is now given by,

$$t = j \tan \left(\frac{\pi f}{2 f_o} \right) \approx j \frac{\pi f}{2 f_o} \quad (26)$$

and assuming that $T_N \left(\cos \frac{\theta}{2} \right) \approx 1$, the transfer function $|S_{21}(\omega)|^2$ may be derived as,

$$|S_{21}(\omega)|^2 \approx A(\omega, Z) \approx \frac{1}{1 + \frac{(Z^2 + 1)^2}{4Z^2} \left(\frac{\pi \omega}{2 \omega_o} \right)^2} \quad (27)$$

where the 3dB point is given by,

$$\omega_{3dB} \approx \frac{4Z\omega_o}{\pi(Z^2 + 1)} \quad (28)$$

Thus except for $f = 2f_o$, $A(\omega, Z)$ becomes relatively small as Z increases which results in a narrower passband bandwidth. Now consider the stopband region where f is around f_o , the control element $A(\omega, Z)$ may be reduced to,

$$A(\omega, Z) \approx \left(\frac{2Z}{Z^2 + 1} \right)^2 \quad (29)$$

as $t \gg 1$. Differentiating $A(\omega, Z)$ with respect to Z gives,

$$\left. \frac{dA(\omega, Z)}{dZ} \right|_{Z=1} = 0 \quad (30)$$

and

$$A_{\max}(\omega, 1) = 1 \quad (31)$$

Thus $A(\omega, Z)$ is always less than unity for $Z \neq 1$ which results in a lower stopband ripple level. Shown in Fig. 5 are the individual responses of the control element and original filter (product of the chebyshev polynomials, $N=2$). The composite transmission response can be obtained by simply summing the individual responses (in dB). Theoretically this type of filter can be designed to have any passband bandwidth and stopband ripple. However, in practice the impedance of the unit element becomes unreasonably high if a very narrow filter bandwidth along with high stopband rejection is required. For example, a 450 Ω impedance line is required to achieve a filter response with 6.75% 3dB bandwidth and -30 dB stopband ripple level.

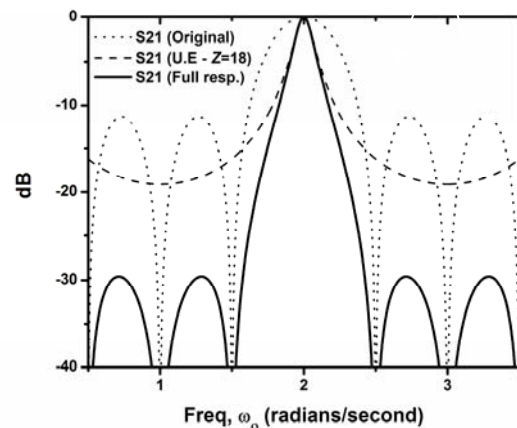


Fig. 5. Original filter and control element responses, and the composite response.

Results

A. Microstrip Prototype

A 2-stage switched delay line tunable filter with scaled impedance was designed and implemented as a hybrid integrated circuit which gives a 2-state response with center frequency at 1.06 GHz and 1.51 GHz. The microstrip circuit prototype is shown in Fig. 6. The power splitters are realized using cascaded three-section Wilkinson dividers in order to cover the required bandwidth. The tuning operation is accomplished by toggling the appropriate position of output switches where the measured results along with the simulated responses of the filter are shown in Fig. 7. The switch elements being used in the design prototypes are Infineon BAR50-02V in SC79 package.

To select state-1 filter response, the diodes D1 are forward biased with 80 mA. In this state, a reverse bias voltage is applied to diodes D2 to disconnect the signal path for state 2. To produce state-2 response centered at 1.51 GHz, diodes D2 are forward biased and D1 are reversed biased. The high impedance quarter-wave-long transmission-line elements of 200 μm -wide microstrip traces are implemented to provide bias to the p-i-n diodes, in conjunction with 150 Ω series resistors, and 100 pF chip capacitors. A maximum passband loss of 1.7 dB across the 35% tuning bandwidth was obtained. The contribution of the switch losses is insignificant ~ 0.6 dB as they were loaded as part of the coupling elements. The passband attenuation is merely attributed to conductor loss.

Four transmission zeros were obtained as expected, yielding a quasi-elliptic response. Minimum stopband rejection level of 17dB was obtained for $Z(\text{unit element})=100 \Omega$. The minor discrepancy between the simulated and measured frequency responses is attributed to small placement error of switch elements.

For linearity validation purpose, two tone

measurement was carried out. Both states produced an IP3 of greater than 32 dBm for input power (0 and 5 dBm) and frequency separation of 50 kHz as shown in Fig. 8.

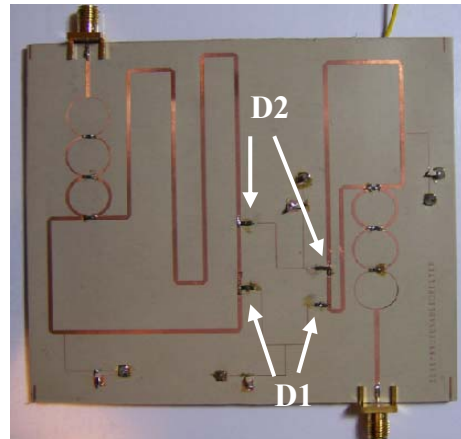


Fig. 6. Microstrip circuit prototype of switched delay line tunable filter with scaled impedance $Z=4$.

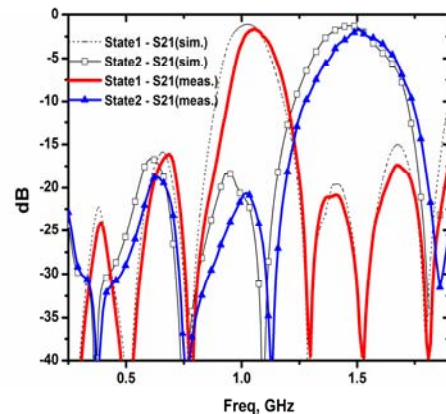


Fig. 7. Simulated and measured transmission responses of switched delay line (SDL) reconfigurable filters.

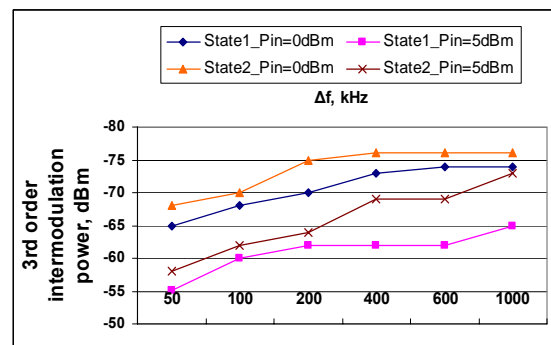


Fig.8. Measured intermodulation power against frequency separation Δf at both states centered at 1.06 and 1.51GHz.

B. Comparison to Conventional Varactor Loaded Comblin Filter

An effort was made to design a tunable filter based on conventional varactor loaded comblin filter topology. A 4-pole microstrip prototype with similar tuning bandwidth was designed and fabricated. Shown in Table 1 are few characteristics of the switched delay line filter compared to the conventional varactor loaded comblin filter. The primary improvements with the proposed reconfigurable filter approach are the excellent linearity performance and low passband loss. Unlike the conventional approach, the variable impedance of the varactor devices is almost transparent to the filter loss performance as the active switch elements are used as part of the coupling elements. In addition a very wide tuning bandwidth is feasible by simply manipulating the phase relationship of parallel delay lines. This approach circumvents the need for varactor devices and offers a significant cost reduction over implementing varactor devices with high capacitance ratio and Q factor.

As for filter performance under large signal conditions, Fig. 9 shows the passband response of the comblin filter as a function of incident signal level. As could be predicted, the passband loss increases with increasing input drive level primarily due to saturation effect of the varactor diodes. The self biasing effect is also evident with high input power. This is basically due to the fact the averaged capacitance values of the varactor's junction diode are different from the respective small signal values, therefore progressively changing the center frequency.

In contrast to conventional approach, the proposed filter has the ability to simultaneously address the loss, distortion and tuning bandwidth issues. However the transfer characteristic of the filter is dominated by the switched delay line and therefore in narrowband applications, phase difference of the delay lines must change

very rapidly with frequency which implies long signal time delays are required. Consequently the space needed to accommodate both stopband and passband bandwidth requirements would become large. To help address this issue, a control element is introduced which could resolve the problem. However the compensation is limited by practical bounds.

Conclusion

A novel electronically tuned microwave filter based on switched delay line approach is proposed and discussed. Theoretical analysis and experimental work are presented. The filter distinguishes itself through its ability to provide 35% tuning range while maintaining a maximum passband loss of 1.7 dB and an IP3 of >32 dBm.

Table 1.

SDL and Tunable Comblin Filter Design Comparison

	SDL	Varactor loaded
Passband loss	~1.7dB	~7dB
IP3	>32dBm	~10dBm
Large signal performance	Good	Poor (suffer from saturation effect and self biasing effect)
Tuning bandwidth	35%	35% (also depends on varactor's cap. ratio)

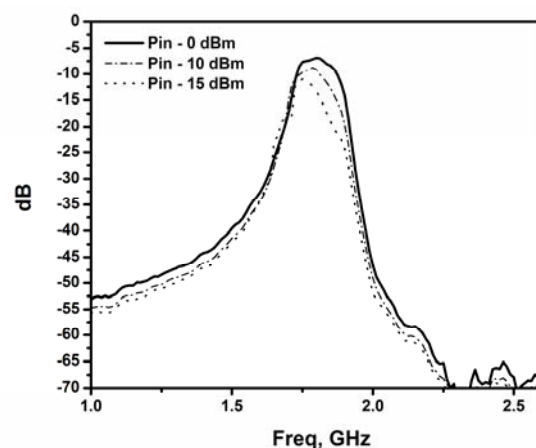


Fig.9. Measured transmission responses of varactor loaded comblin filter with increasing input drive level.

Acknowledgment

The work reported in this paper was funded by the Electro-Magnetic Remote Sensing (EMRS) Defence Technology Centre, established by the UK Ministry of Defence and run by a consortium of SELEX Galileo, Thales UK, Roke Manor Research and Filtronic.

References

1. I. C. Hunter, Theory and Design of Microwave Filters, IEE, London, UK:2001, pp. 194, 325.
2. J. S. Hong, M. J. Lancaster, Microstrip filters for RF/microwave applications, New York, Wiley, 2001.
3. Hector J. De Los Santos, RF MEMS circuit design for wireless communications, London, Artech House, 2002.
4. Pothier, J. C. Orlianges, Z. Guizhen, C. Champeaux, A. Catherinot, D. Cros, P. Blondy, and J. Papapolymerou, "Low-loss 2-bit tunable bandpass filters using MEMS DC contact switches," Microwave Theory and Techniques, IEEE Transactions on, vol. 53, pp. 354-360, 2005.
5. K. Entesari and G. M. Rebeiz, "A differential 4-bit 6.5-10-GHz RF MEMS tunable filter," Microwave Theory and Techniques, IEEE Transactions on, vol. 53, pp. 1103-1110, 2005.
6. Abbaspour-Tamijani, L. Dussopt, and G. M. Rebeiz, "Miniature and tunable filters using MEMS capacitors," Microwave Theory and Techniques, IEEE Transactions on, vol. 51, pp. 1878-1885, 2003.
7. J. Nath, D. Ghosh, J. P. Maria, A. I. Kingon, W. Fathelbab, P. D. Franzon, and M. B. Steer, "An electronically tunable microstrip bandpass filter using thin-film Barium-Strontium-Titanate (BST) varactors," Microwave Theory and Techniques, IEEE Transactions on, vol. 53, pp. 2707-2712, 2005.
8. J. Nath, W. M. Fathelbab, P. G. Lam, D. Ghosh, S. Aygun, K. G. Gard, J. P. Maria, A. I. Kingon, and M. B. Steer, "Discrete Barium Strontium Titanate (BST) Thin-Film Interdigital Varactors on Alumina: Design, Fabrication, Characterization, and Applications," IEEE MTT-S Int. Microw. Symp. Dig., 2006.
9. I. C. Hunter, S. R. Chandler, "Intermodulation distortion in active microwave filters," IEE Proc. Microwave, Antennas and Propagation., vol. 145, no. 1, pp. 7-12, Feb 1998.
10. C. Rauscher, "Varactor-tuned notch filter with low passband noise and signal distortion," IEEE Trans. Microwave Theory and Techniques., vol. 49, no. 8, pp. 1431-1437, Aug 2001.
11. H. Trabelsi and C. Cruchon, "A varactor-tuned active microwave bandpass filter," Microwave and Guided Wave Letters, IEEE, vol. 2, pp. 231-232, 1992.
12. S. R. Chandler, I. C. Hunter, and J. G. Gardiner, "Active varactor tunable bandpass filter," Microwave and Guided Wave Letters, IEEE, vol. 3, pp. 70-71, 1993.
13. D. R. Jachowski, "Compact, frequency-agile, absorptive bandstop filters," IEEE MTT-S Int. Microw. Symp. Dig., 2005.